

# Effect Of Boundary Conditions On Shear Banding In True Triaxial Tests On Sand

P.V. Lade<sup>1</sup> and Q. Wang<sup>2</sup>

<sup>1</sup>Department of Civil Engineering, The Catholic University of America, Washington, D.C., U.S.A.

<sup>2</sup>RJM Engineering, Inc., Ellicott City, MD, U.S.A.

E-mail: Lade@cua.edu

**ABSTRACT:** Shear banding in true triaxial tests on sand have been studied to determine its effects on failure under three-dimensional conditions. Experiments have been performed on rectangular prismatic specimens with height-to-diameter ratio  $H/D = 2.47$  and on cubical specimens with  $H/D = 1.0$  to determine the influence of slenderness ratio and stiff versus soft boundaries on the results of such tests. The experiments show clear differences between the two types of tests: Shear banding in the tall specimens occurs with a sharp peak, while the short specimens show smoother stress-strain behavior near the peak, and all friction angles from the short specimens are 1-2 degrees higher than those from the tall specimens. The analysis of shear banding indicates that the critical hardening moduli are closer to zero for the short specimens than for the tall specimens. Indications are that experiments should be performed on tall specimens in which the shear banding occurs freely, while the short specimens impede and delay the development of shear bands.

## 1. INTRODUCTION

Several series of true triaxial tests have been performed on cubical and rectangular prismatic specimens of Santa Monica Beach sand at three different relative densities to study the occurrence of failure, the mechanisms that create failure, and the soil behavior in the vicinity of failure. One mechanism is smooth peak failure, in which the soil continues to behave as a continuum with uniform strains, and smooth peak failure is followed by strain softening. Another mechanism is shear banding whose occurrence in the plastic hardening regime limits the strength of the soil. Presented here are analyses based on theoretical conditions for localization and subsequent shear banding and on results of true triaxial tests on tall and short specimens. Of special interest is the influence of specimen slenderness on the three-dimensional sand behavior. While the short specimens tend to impede the strain localization, shear banding does occur approximately in the same interval of  $b = (\sigma_2 - \sigma_3) / (\sigma_1 - \sigma_3)$ , but at higher strengths than obtained for the tall specimens.

## 2. PREVIOUS STUDIES

Experimental results with respect to the formation of shear banding under generalized principal stress conditions are available from only few previous studies (e.g. Arthur et al. 1977; Arthur and Dunstan 1982; Vardoulakis 1980; Desrues et al. 1985, 1996; Yoshida et al. 1993; Yoshida and Tatsuoka 1997; Finno et al. 1996, 1997; Oie et al. 2003). The stress-strain relations obtained from true triaxial tests commonly show continuously decreasing strain-to-failure, and more pointed peaks with increasing  $b$ -value near and greater than the value at plane strain. The rapid decline in strength after peak failure may suggest that shear banding occurs in the hardening regime, i.e. on the way up to smooth peak failure, and that it is prevalent over a wide range of  $b$ -values. Therefore, failure may be a consequence of the development of shear bands in the hardening regime for this range of  $b$ -values, and the peak strength may be dependent on the critical condition in the hardening regime at which shear banding occurs.

Based on theoretical considerations, Rudnicki and Rice (1975) and Rice (1976) suggested a range of stress states in which the hardening modulus, critical for strain localization and subsequent shear banding, is positive, i.e. shear banding may occur during increasing loading before smooth peak failure has been reached, as shown in Figures. 1 and 2. According to these schematic diagrams, shear banding may occur in the hardening regime in the mid-range of  $b$ -values, whereas it may occur for negative critical hardening moduli, i.e. in the softening regime, for  $b$ -values at and in the vicinity of triaxial compression and triaxial extension.

True triaxial equipment that produces uniform stresses and strains and covers the full range of variation of the intermediate principal stress is required to establish the influence of shear banding on the three-dimensional stress-strain and strength behavior of sand.

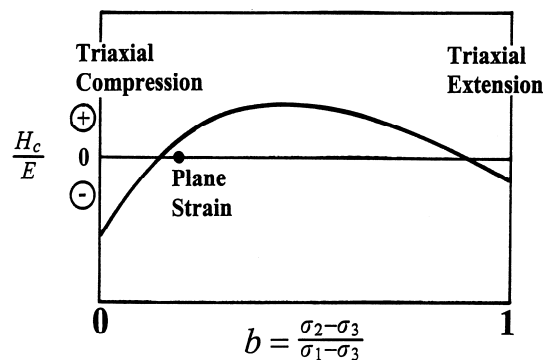


Figure 1. Schematic diagram of variation of normalized, critical hardening modulus with  $b$  according to Rudnicki and Rice (1975) and Rice (1976).

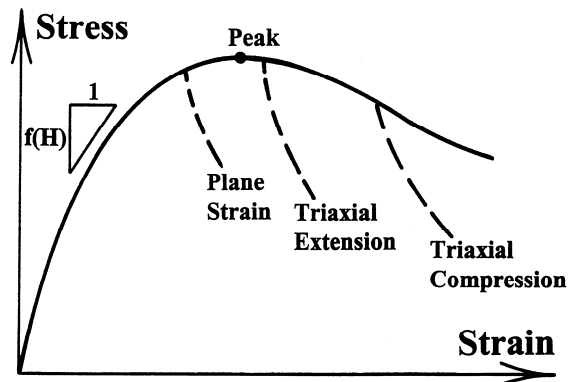


Figure 2. Generic stress-strain relation indicating occurrence of shear banding relative to smooth peak failure for different 3-D stress conditions according to Rudnicki and Rice (1975) and Rice (1976).

## 3. EXPERIMENTS

Experiments have been performed in a true triaxial apparatus on Santa Monica Beach sand. The cubical triaxial apparatus, shown in Figure 3 and previously described by Lade and Duncan (1973), was modified to accommodate specimens with a height-to-diameter ratio  $H/D = 2.47$ , and experiments were also performed with  $H/D = 1.0$  to study the influence of slenderness ratio and stiff versus soft boundaries on shear banding under three-dimensional conditions.

Soft boundaries are provided by the latex rubber membrane used to surround the specimen in conventional triaxial tests. Shear bands are not impeded, because this boundary is sufficiently flexible to

allow their development. Stiff boundaries are provided by the cap and base, and they are also provided by the stiff, vertically compressible side plates employed in the true triaxial apparatus shown in Figure 3. These boundaries impede, but do not prevent the development of shear bands. Thus, the shear bands develop later in experiments in which they tend to intersect the stiff end plates, as explained in detail in sections 5 and 6.

Figure 4 shows a schematic diagram of how the shear band development is impeded by the stiff end plates in the short specimen, while the soft rubber membrane surrounding the tall specimen allows the shear band to develop freely. Note that the stiff side plates, which provide the second deviator stress ( $\sigma_2 - \sigma_3$ ) in the true triaxial apparatus, do not interfere with the development of shear bands, which occur in the 1-3 plane for an isotropic material.

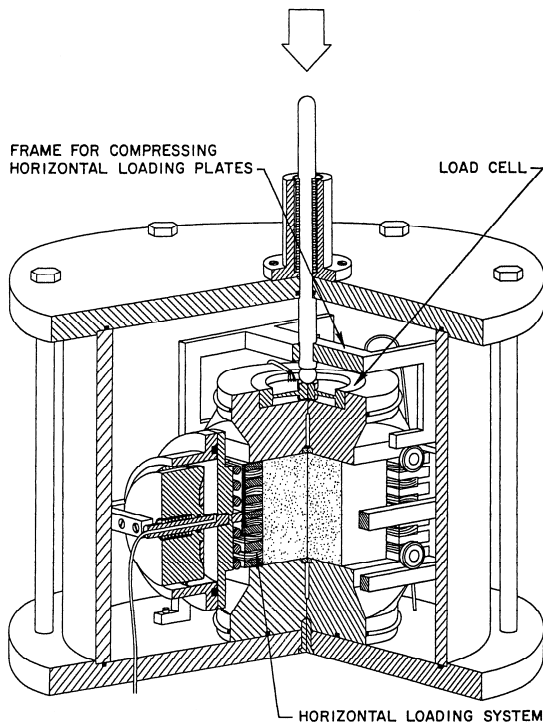


Figure 3. Cubical triaxial apparatus.

### 3.1 Experimental Procedures

The Santa Monica Beach sand employed in the experiments is composed of angular to subangular particles consisting of 45% quartz, 45% feldspar, 8% magnetite and 2% trace minerals. The characteristics of this sand are summarized as follows: Mean diameter, 0.25 mm; coefficient of uniformity, 1.69; specific gravity of grains, 2.66; maximum void ratio, 0.91; and minimum void ratio, 0.60. Experiments were performed on specimens with void ratios of 0.63, 0.68, and 0.76 corresponding to relative densities of 90% (dense), 74% (medium dense), and 50% (loose).

Both the tall prismatic and the cubical specimens were prepared by dry pluviation using different fall heights, as described by Wang and Lade (2001). This method of sand deposition produces inherent cross-anisotropy with horizontal bedding planes and a vertical axis of material symmetry in the specimens. However, all tests were performed in sector I of the octahedral plane in which the effects of cross-anisotropy are not pronounced. Additional tests on tall and short specimens in sectors II and III are required to obtain the complete picture of effects of boundary conditions on shear banding in cross-anisotropic sand deposits. Lam and Tatsuoka ((1988a and b) performed triaxial compression ( $b = 0$ ) and extension tests ( $b = 1$ ) on specimens with bedding planes oriented horizontally and vertically, thus studying the strength and deformation characteristics of sand as affected by cross-anisotropy.

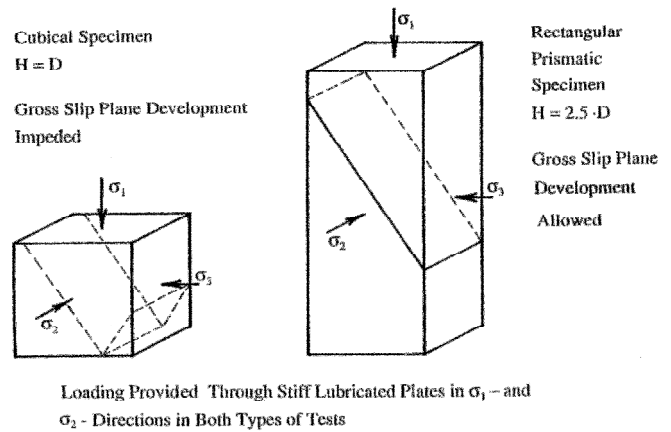


Figure 4. Effect of boundary conditions on development of shear bands in true triaxial tests with different slenderness ratios.

The specimens created by dry pluviation of Santa Monica Beach sand were saturated with water employing the CO<sub>2</sub>-method described in detail by Lade and Duncan (1973). The three-dimensional experiments were performed with a constant effective confining pressure of  $\sigma_3' = 49$  kPa and constant target values of  $b = 0.0, 0.1, 0.15, 0.2, 0.3, 0.4, 0.5, 0.6, 0.7, 0.8, 0.9,$  and  $1.0$ .

### 4. EXPERIMENTS ON TALL SPECIMENS

Wang and Lade (2001) presented results of experiments on tall prismatic specimens. The key diagrams for the tall specimens are presented here for comparison with the results of short specimens. The stress-strain curves for dense sand are compared in Figure 5, and all failure surfaces are shown in Figure 6. They strongly indicate an influence of shear banding in the hardening regime on the peak strength of the material under three-dimensional stress conditions in the midrange of  $b$ -values, including the plane strain condition.

The strength under three-dimensional stress conditions does not increase continuously with  $b$ , nor does it increase to the plane strain condition and decrease afterwards as reported by many previous investigators. It is found in this experimental study that the strength increases as  $b$  increases from 0 to about 0.18, then remains almost constant or even decreases slightly for  $b$  in the range of 0.18 - 0.40. For  $b$  greater than 0.40, the strength increases slowly until  $b$  reaches 0.85, and then decreases slightly to  $b = 1.0$ .

The strain-to-failure decreases rapidly with increasing value of  $b$  for low  $b$ -values. For  $b$  greater than 0.3, the strain-to-failure remains almost constant until  $b$  reaches unity. The maximum rate of dilation varies only little for low values of  $b$ , but then increases monotonically until  $b$  reaches unity, where the rate of dilation is approximately two times the rate observed at  $b = 0.0$  (Wang and Lade, 2001).

The softening observed after shear banding is initiated occurs along a reasonable constant slope, which is dependent on the mean grain size, as observed by Yoshida and Tatsuoka (1997) and Oie et al (2003). This slope or rate of strength declination is steeper than the material softening occurring during homogeneous deformation in the softening regime following smooth peak failure and it is therefore easily detectable, as shown in Figure 5. The homogeneous strain softening occurs because the void ratio continues to increase due to dilation and the peak strength consequently decreases. In comparison, the softening due to shear banding occurs faster because the deformation is localized in the shear band, and the linear axial strains are not homogeneous inside the entire specimen, but represents the deformation occurring in the shear band. The axial strains are therefore affected by the highly non-homogeneous deformations after the shear band has developed, and this shows up in the stress-strain relation as a specimen size effect.

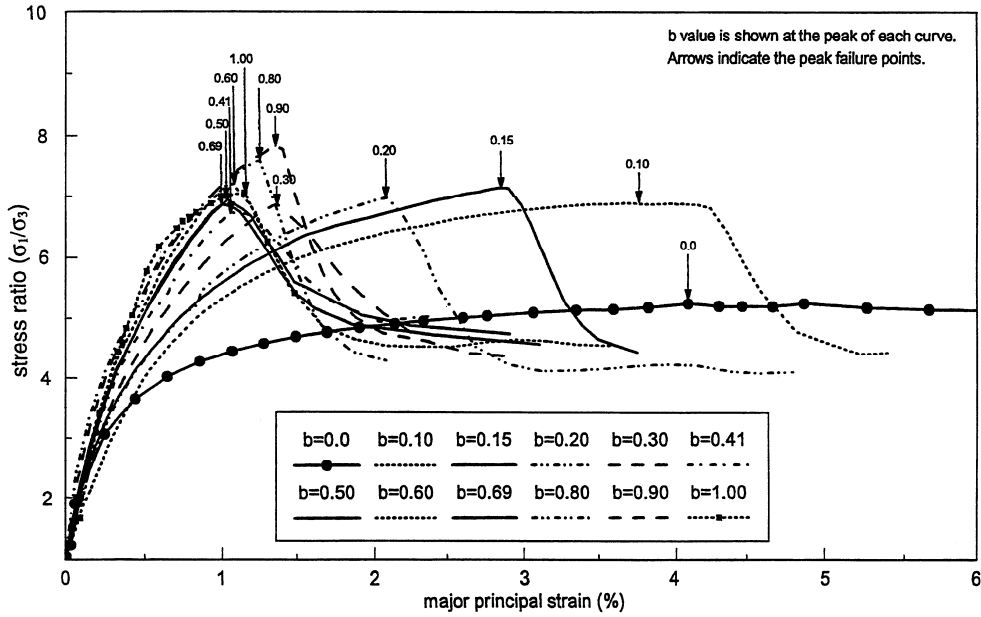


Figure 5. Comparison of stress ratio-strain characteristics in true triaxial tests on tall prismatic specimens of dense Santa Monica Beach sand with  $\sigma_3' = 49$  kPa.

Shear banding, detected through the abrupt slope change of the  $\epsilon_1 - \epsilon_2$  curve and the sudden strength reduction, initiates in the hardening regime when  $b$  is in the approximate range of 0.18 - 0.85. Failure in these tests is considered to be a consequence of shear banding rather than a continuum response. Thus, peak failure is caused by shear banding in this middle range of  $b$ -values, and a smooth, continuous three-dimensional failure surface is therefore not obtained in general for soils.

To verify this, the condition for shear band formation proposed by Rudnicki and Rice (1975) was examined for each test through the computation of the hardening modulus prior to onset of shear banding. This hardening modulus was calculated for each test using the following expression (Lade and Wang, 2001):

$$H = \frac{\left( \frac{\partial f}{\partial \sigma_1} \Delta \sigma_1 + \frac{\partial f}{\partial \sigma_2} \Delta \sigma_2 + \frac{\partial f}{\partial \sigma_3} \Delta \sigma_3 \right)}{\sqrt{\left( \frac{\partial f}{\partial \sigma_1} \right)^2 + \left( \frac{\partial f}{\partial \sigma_2} \right)^2 + \left( \frac{\partial f}{\partial \sigma_3} \right)^2}} \cdot \frac{1}{\sqrt{\left( \Delta \epsilon_1^p \right)^2 + \left( \Delta \epsilon_2^p \right)^2 + \left( \Delta \epsilon_3^p \right)^2}} \quad (1)$$

where the increments in normal stresses,  $(\Delta \sigma_1, \Delta \sigma_2, \Delta \sigma_3)$ , and normal strains,  $(\Delta \epsilon_1^p, \Delta \epsilon_2^p, \Delta \epsilon_3^p)$ , are those measured immediately before the shear band development in the true triaxial tests. Note that the confining pressure was always constant in the true triaxial tests presented here and therefore  $\Delta \sigma_3 = 0$ . The other increments in stresses and plastic strains may be determined from the slopes of the stress-strain relations immediately prior to the development of the shear bands.

The expression in Eq. (1) is general and therefore applicable for any constitutive model with a yield function  $f$ . To calculate the hardening modulus from Eq. (1), a specific function has to be assumed. In the analyses performed by Lade and Wang (2001), the yield function proposed by Lade and Kim (1988) was employed.

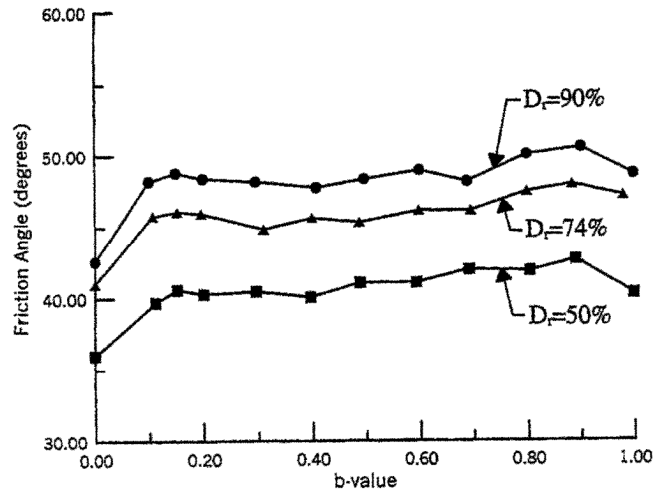


Figure 6. Variation in friction angle with  $b$ -value for true triaxial tests on tall prismatic specimens on dense, medium dense, and loose Santa Monica Beach sand with  $\sigma_3' = 49$  kPa.

This yield function is given by the expression:

$$f = \left( \psi_1 \cdot \frac{I_1^3}{I_3} - \frac{I_1^2}{I_2} \right) \cdot \left( \frac{I_1}{p_a} \right)^h \cdot e^q \quad (2)$$

in which  $I_1, I_2,$  and  $I_3$  are the three invariants of the stress tensor and  $\psi_1, h,$  and  $q$  are soil parameters to be determined as explained by Kim and Lade (1988) and Lade and Kim (1988). The yield surface depicted by Eq. (2) traces a surface of constant plastic work as measured from the stress origin. In principal stress space, it is shaped as an asymmetric teardrop with a smoothly rounded triangular cross-section.

Using the expression for the yield surface in Eq. (2), the experimental, normalized, critical, hardening moduli obtained from Eq. (1) are presented in Figure 7. This diagram shows that for  $b$ -values in the ranges from 0 to 0.18 and from 0.85 to 1.0, negative hardening moduli were obtained, implying that conditions for shear

band formation are fulfilled in the softening regime. Therefore, failure occurs by smooth peak failure and as a continuum response in these ranges. Positive values of the hardening moduli immediately before onset of shear banding was obtained when  $b$  was in the approximate range of 0.18 - 0.85, indicating that the condition for bifurcation is fulfilled in the hardening portion of stress-strain curve. Thus, peak failure is caused by shear banding in this middle range of  $b$ -values, and a smooth, continuous three-dimensional failure surface is therefore not obtained in general for soils.

**5. EXPERIMENTS ON SHORT SPECIMENS**

To determine the effects of slenderness ratio on the occurrence of shear banding, if any, the experiments performed on tall specimens were repeated on cubical specimens with  $H/D = 1.0$ . The patterns of variations of the strength, the strain-to-failure, the rate of dilation, and the relations between principal strains were basically the same for the short and the tall specimens. Figures. 8 and 9 show representative comparisons of stress-strain and volume change relations for tall and short specimens of medium dense sand at  $b = 0.40$  and  $0.80$ , respectively. Very similar behavior was produced in the specimens before failure occurred. The only difference in response of the two specimens before failure was observed in the volume change behavior. The short specimens dilated a little more than the tall specimens, indicating a slightly higher degree of uniformity of deformation in the short specimens. The tall specimens, in which shear banding was free to develop, failed earlier, and their strengths dropped more rapidly after failure than in the short specimens. Development of shear bands were impeded in the short specimens, thus delaying the occurrence of and increasing the peak stress ratio, as indicated in Figures. 8 and 9. The condition of zero volume change and zero strength reduction was reached within much smaller amounts of post-peak straining for the tall specimens, while the short specimens in which uniformity of deformation was maintained longer also produced higher residual strengths than the tall specimens. This may also be seen by comparison of the stress-strain curves in Figure 5 for tall specimens and in Figure 10 for short specimens of dense sand.

Figure 11 shows the critical hardening moduli calculated from the stress-strain curves for short specimens of dense sand shown in Figure 10. Comparison of Figures. 7 and 11 indicates that the hardening moduli for short specimens are lower in the hardening regime and higher in the softening regime, i.e. they are closer to zero than those for the tall specimens.

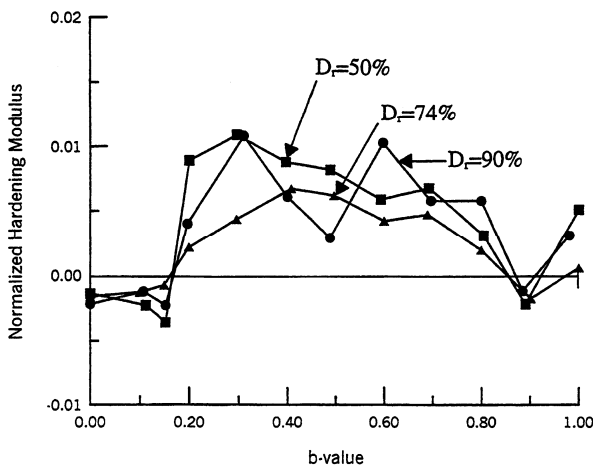


Figure 7. Variation of normalized, critical hardening modulus,  $H_c/E$ , with  $b$  for true triaxial tests on tall prismatic specimens on dense, medium dense, and loose Santa Monica Beach sand with  $\sigma_3' = 49$  kPa.

**6. EFFECTS OF BOUNDARY CONDITIONS**

Shear bands in specimens with  $H/D = 1.0$  always intersect the lubricated cap and base, while they are free to develop through the soft membrane in the specimens with  $H/D = 2.47$ . There is a tendency for visible onset of shear banding slightly after the peak stress point in the short specimens, as shown in Figure 7, while failure and shear banding occur simultaneously in the tall specimens. Intersection of shear bands with the end plates enhances uniform strains, also well before any gross shear banding develops in the short specimens. This is also indicated by the higher rates of dilation in the short specimens before shear banding develops, as shown in Figures 8 and 9.

This tendency for short specimens to produce more uniform deformations favors their use in research investigations. Such investigations are often performed in triaxial compression for which the shear banding occurs in the softening regime. Therefore, shear banding plays no role in the quality of the triaxial compression test, and it is considered advantageous to enforce uniform strains in tests on short specimens.

With the help of photogrammetric techniques, Desrues et al. (1985), Yoshida et al. (1993), and Finno et al. (1996, 1997) observed strain localization developing along directions of potential shear bands in specimens under plane strain conditions before the peak state. This may imply that strain localization to a certain degree commonly occurs in specimens before failure. The rigid boundaries of the short specimen may effectively prevent the more strained regions from evolving into shear bands and hence enforce macroscopically more uniform deformations than in the tall specimen. Further, evolution of a shear band in a short specimen requires that it be reflected from the stiff, smooth boundaries and advances into another region before its full zig-zag development throughout the specimen.

However, the tendency of the stiff, smooth plates to delay the onset of strain localization and subsequent shear banding and to smooth out the stress-strain relations around the peak point in the middle range of  $b$ -values may be problematic. It may not represent a continuum response, but rather a conglomerate of incipient shear banding and compression of the sharp points between shear bands near the stiff, lubricated ends.

Therefore, the occurrence of the critical conditions for bifurcation throughout the sand may be delayed in a short specimen, and the stress state may, in fact, become over-critical in some portions before the short specimen shows indications of shear banding and failure. In comparison, the effects of restraints from the stiff, lubricated boundaries on the uniformity of deformation in a tall specimen are much less pronounced, and the critical stress state for bifurcation may be reached in a tall specimen at a smaller average strain. A single shear band can develop rather freely in a tall specimen. Hence the tall specimen shows earlier and more pronounced softening behavior.

Failure and softening behavior is closely related with shear banding. For a specimen that fails by smooth peak failure under homogeneous conditions, as in triaxial compression ( $b = 0.0$ ), the stress-strain behavior in the softening regime consists of three stages: Material softening, shear band softening, and the residual state. During the first stage, the strength decreases slowly from the peak and the  $\epsilon_2$ - $\epsilon_1$  relationship continues to develop as an essentially linear relation. As the specimen enters the strain localization and shear band softening stage, deformation becomes localized in the shear band. The strength decreases abruptly, and the development of the intermediate principal strain,  $\epsilon_2$ , also abruptly reduces to zero in both the tall and the short specimens. Finally, a well-defined shear band forms, and the residual state is reached, indicated by termination of (1) strength reduction, (2) development of intermediate principal strain, and (3) development of volume change.

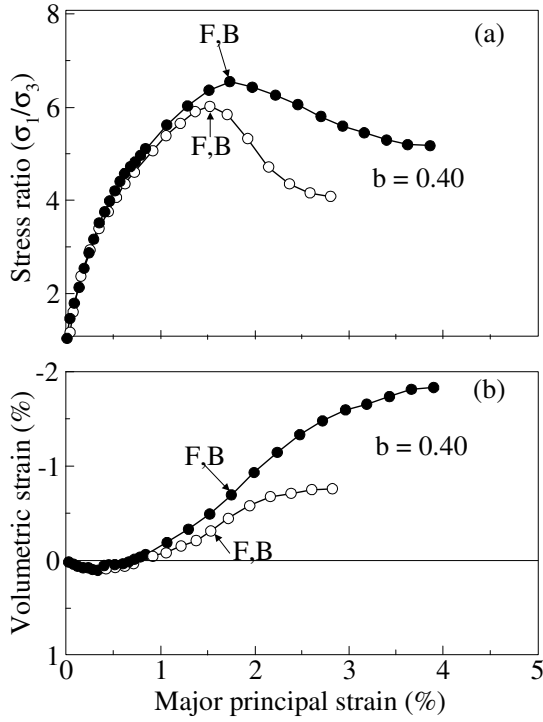


Figure 8. Comparison of stress-strain and volume change characteristics for short and tall prismatic, medium dense specimens at  $b = 0.40$ . Open points indicate a short specimen with  $H = D$ , and solid points are for a tall specimen with  $H = 2.47D$ .

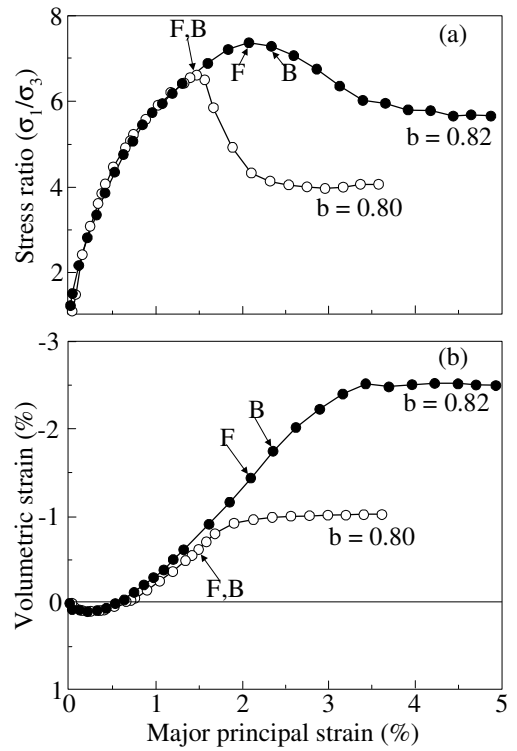


Figure 9. Comparison of stress-strain and volume change characteristics for short and tall prismatic, medium dense specimens at  $b = 0.80-0.82$ . Open points indicate a short specimen with  $H = D$ , and solid points are for a tall specimen with  $H = 2.47D$ .

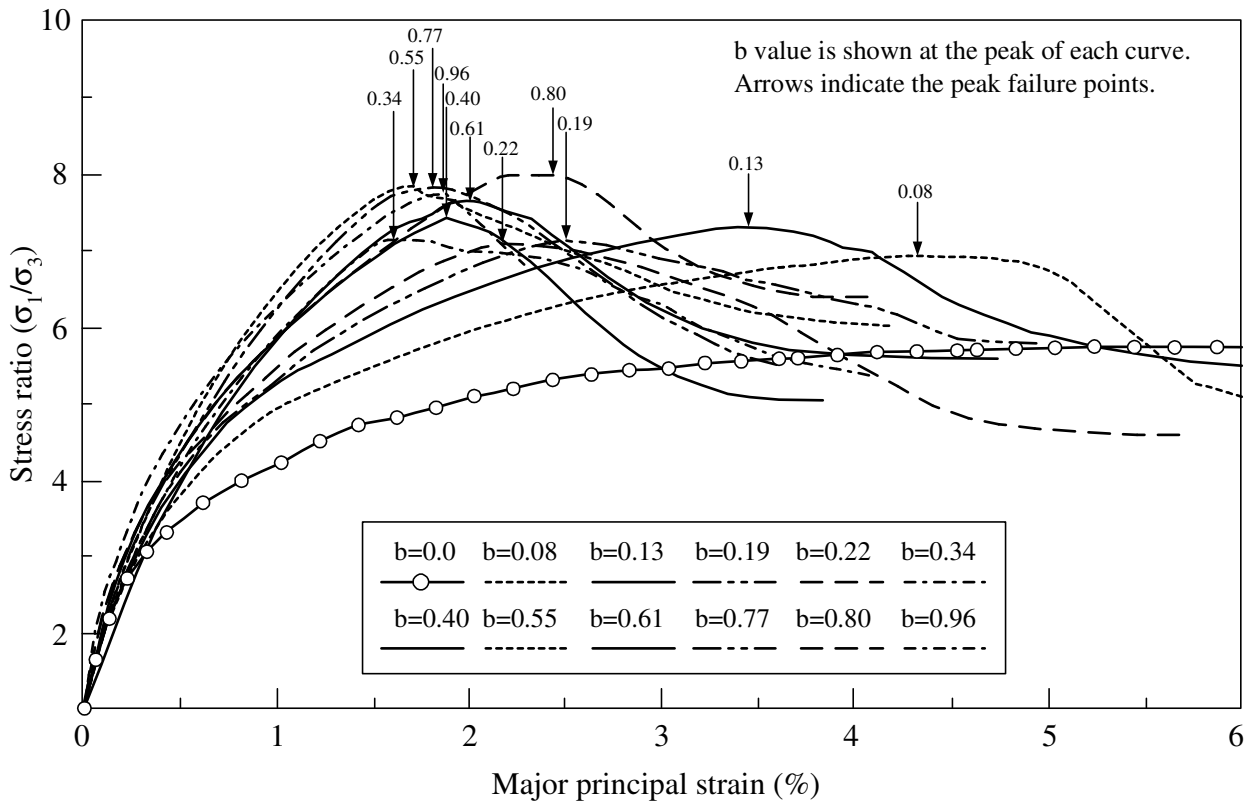


Figure 10. Comparison of stress ratio-strain characteristics in true triaxial tests on short prismatic specimens of dense Santa Monica Beach sand with  $\sigma'_3 = 49$  kPa.

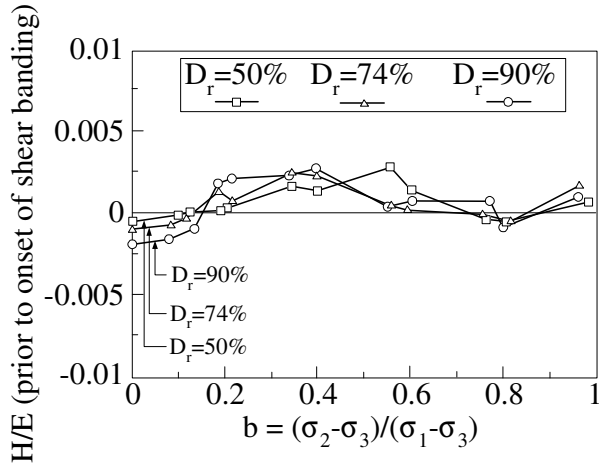


Figure 11. Variation of normalized, critical hardening modulus,  $H/E$ , with  $b$  for true triaxial tests on short prismatic specimens of dense, medium dense, and loose Santa Monica Beach sand with  $\sigma_3' = 49$  kPa.

For a test in which shear banding develops in the hardening regime, softening consists of two stages only: Shear band softening and residual state. A material softening stage does not exist. Shear band softening starts right after peak failure.

Figure 12 shows a comparison of friction angles for true triaxial tests on short and tall specimens for all three relative densities. The friction angles are generally 1-2 degrees higher in the short specimens, with the smallest differences obtained in the triaxial compression tests. The occurrence of shear banding in the hardening regime induced failure in the range of  $b$ -values from 0.18 to 0.85 in the tall specimens, while they occurred in the range from 0.13 to 0.75 in the short specimens.

Thus, the stiff, smooth boundaries in the short specimens were able to delay the onset, but they were not able to prevent the shear banding phenomenon. Outside the middle range of  $b$ -values, shear banding occurred in the softening regime, and failure expressed itself as a smooth peak response. Instead of ascending continuously as  $b$  increases, the  $\phi - b$  curves become concave as the experiments are influenced by early shear banding.

### 7. SHEAR B AND INCLINATION

The slenderness ratio was  $H/D = 2.47$  for the tall rectangular prismatic specimens, and this allowed the free development of shear bands without interference with the lubricated ends. The angles of shear band inclination with respect to the  $\sigma_1$ -plane were measured in the experiments, and with few exceptions the inclinations varied essentially between  $60^\circ$  and  $70^\circ$ . They were not much affected by the values of  $b$ , but they increased slightly with increasing density.

Figure 13 shows comparisons between the measured shear band inclinations in the tall specimens with three different relative densities. They are compared with the inclinations predicted on the basis of (1) Coulomb's theory,  $\alpha = 45^\circ + \phi/2$ , (2) Roscoe's considerations of strains (Roscoe 1970),  $\alpha = 45^\circ + \psi/2$ , and (3) Arthur's proposal (Arthur et al. 1977; Arthur and Dunstan 1982),  $\alpha = 45^\circ + (\phi + \psi)/4$ . Fig. 13 indicates that the experimental observations are located between the Coulomb and the Arthur inclinations, but are closer to the Coulomb inclination angle for all true triaxial tests except triaxial compression ( $b = 0$ ) for which the inclination is closest to that proposed by Arthur. However, to be certain to avoid interference of the stiff cap and base with development of shear bands, the specimen height should be  $H > D \cdot \tan(45^\circ + \phi/2)$ .

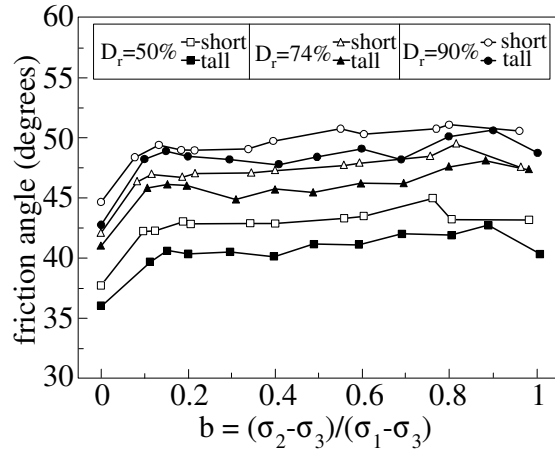


Figure 12. Comparison of friction angles for true triaxial tests on short and tall prismatic specimens of dense, medium dense, and loose Santa Monica Beach sand with  $\sigma_3' = 49$  kPa.

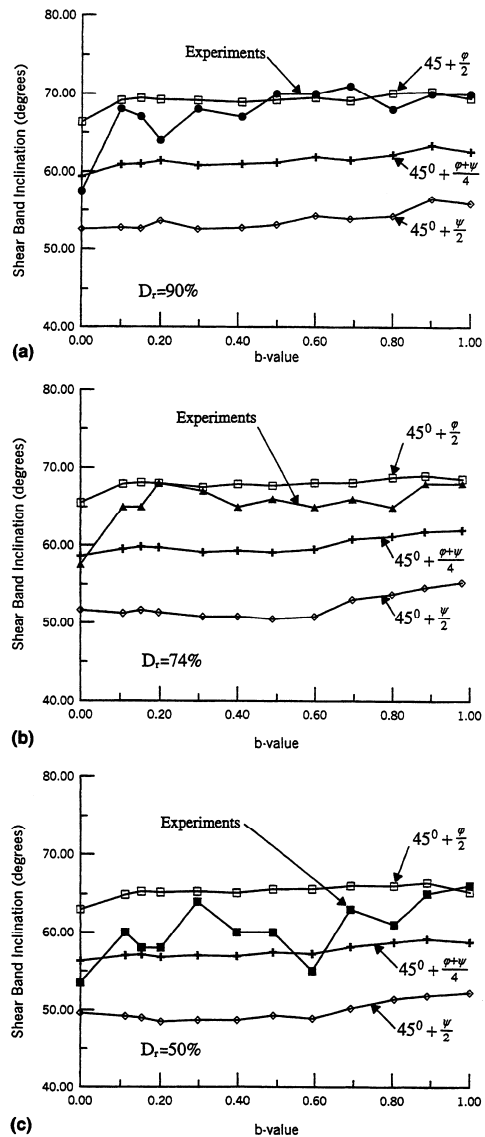


Figure 13. Experimental shear band inclinations compared with three theoretical values for Santa Monica Beach sand: (a) dense, (b) medium dense, and (c) loose.

## 8. CONCLUSION

An experimental investigation of the effect of specimen slenderness ratio on shear banding under three-dimensional conditions has been performed on specimens of sand in a true triaxial apparatus. For all three relative densities tested, the results show that shear banding initiates in the hardening regime when  $b$  is in the approximate range of 0.18 - 0.85 for tall specimens and in the approximate range of 0.13 - 0.75 for the short specimens. While the use of stiff, lubricated ends was able to delay the onset of shear banding in the short specimens, the shear banding phenomenon could not be prevented, but a slight shift of the range of  $b$ -values in which shear banding occurred in the hardening regime was possible. However, peak failure is caused by shear banding in the middle range of  $b$ -values, and a smooth, continuous 3D failure surface is therefore not generally obtained for soils. The experiments show clear differences between the tall and the short specimens: Shear banding in the tall specimens occurs with a sharp peak, while the short specimens tend to impede the strain localization and they show more smooth stress-strain behavior near the peak. All friction angles from the short specimens are 1-2 degrees higher than those from the tall specimens for all three relative densities of the sand.

Inclinations of shear bands in the true triaxial tests were measured and compared with those associated with Coulomb's theory and those proposed by Roscoe and by Arthur. The experiments appear to produce shear band inclinations that are best described by the Coulomb theory. Thus, shear bands in Santa Monica Beach sand tend to form angles with the plane of the major principal stress of  $45^\circ + \phi/2$ .

## 9. REFERENCES

- Arthur, J.R.F., and Dunstan, T. (1982) "Rupture layers in granular media," *Proceedings, IUTAM Symposium on Deformation and Failure of Granular Materials, Delft*, P.A. Vermeer and H.J. Luger, Eds. Balkema, Rotterdam, pp 453-459.
- Arthur, J.R.F., Dunstan, T. Al-Ani, Q.A.J.L., and Assadi, A. (1977) "Plastic deformation and failure in granular media," *Geotechnique*, 27(1), pp 53-74.
- Desrues, J., Lanier, J., and Stutz, P. (1985) "Localization of the deformation in tests on sand sample." *Engineering Fracture Mechanics*. 21(4), pp 909-921.
- Desrues, J., Chambon, R. Mokni, M. And Mazerolle, F. (1996) "Void ratio evolution inside shear bands in triaxial sand specimens studied by computed tomography," *Geotechnique*, 46(3), pp 529-546.
- Finno, R. J., Harris, W. W., Mooney, M. A., and Viggiani, G. (1996) "Strain Localization and undrained steady state of sand." *J. of Geotech. Engrg.*, 122(6), pp 462-473.
- Finno, R. J., Harris, W. W., Mooney, M. A., and Viggiani, G. (1997) "Shear bands in plane strain compression of loose sand." *Geotechnique*, 47(1), pp 149-165.
- Kim, M.K., and Lade, P.V. (1988) "Single Hardening Constitutive Model for Frictional Materials, I. Plastic Potential Function," *Computers and Geotechnics*, 5, pp 307-324.
- Lade, P. V., and Duncan, J. M. (1973) "Cubical triaxial tests on cohesionless soils." *Journal of the Soil Mechanics and Foundation Division, ASCE*, 99(SM10), pp 793-812.
- Lade, P.V., and Kim, M.K. (1988) "Single Hardening Constitutive Model for Frictional Materials, II. Yield Criterion and Plastic Work Contours," *Computers and Geotechnics*, 6, pp 13-29.
- Lade, P.V., and Wang, Q. (2001) "Analysis of Shear Banding in True Triaxial Tests on Sand," *Journal of Engineering Mechanics, ASCE*, 127(8), pp 762-768.
- Lam, W.K., and Tatsuoka, F. (1988a) "Effects of Initial Anisotropic Fabric and  $\sigma_2$  on Strength and Deformation Characteristics of Sand," *Soils and Foundations*, 28(1), pp 89-106.
- Lam, W.K., and Tatsuoka, F. (1988b) "Triaxial Compressive and Extension Strength of Sand Affected by Strength Anisotropy and Sample Slenderness," *Advanced Triaxial testing of Soil and Rock, ASTM STP 977*, R. T. Donaghe, R.C. Chaney, and M.L. Silver, Eds. American Society for Testing and Materials, West Conshohocken, PA, p 655-666.
- Oie, M., Sato, N., Okuyama, Y., Yoshida, Teru, Yoshida, Tatsuya, Yamada, S., and Tatsuoka, F. (2003) "Shear banding characteristics in plane strain compression of granular materials," *Proceedings of the 3<sup>rd</sup> International Symposium on Deformation Characteristics of Geomaterials*, Lyon, France, I, pp 597-606.
- Roscoe, K.H. (1970) "The influence of strains in soil mechanics." *Geotechnique*, 20(2), pp 129-170.
- Rice, J.R. (1976) "The localization of plastic deformation," *Proceedings of the Fourth Conference on Theoretical and Applied Mechanics*, Edited by W.T. Koiter, North-Holland Publishing Co. Amsterdam, pp 207-229.
- Rudnicki, J. W., and Rice, J. R. (1975) "Conditions for the localization of deformation in pressure-sensitive dilatant materials." *Journal of Mech. Phys. Solids*, 23, pp 371-394.
- Vardoulakis, I. (1980) "Shear band inclination and shear modulus of sand in biaxial tests," *International Journal for Numerical and Analytical Methods in Geomechanics*, 4, pp 103-119.
- Wang, Q., and Lade, P.V. (2001) "Shear banding in true triaxial tests and its effect on failure in sand." *Journal of Engineering Mechanics, ASCE*, 127(8), pp 754-761.
- Yoshida, T., and Tatsuoka, F. (1997) "Deformation property of shear band in sand subjected to plane strain compression and its relation to particle characteristics," *Proceedings of the 14<sup>th</sup> International Conference on Soil Mechanics and Foundation Engineering, Hamburg*, Vol. 1, pp 237-240.
- Yoshida, T., Tatsuoka, F., Siddiquee, M. S. A., Kamegai, Y., and Park, C.-S. (1993) "Shear banding in sands observed in plane strain compression." *Proc. 3rd int. Workshop Localisation and Bifurcation Theory for Soils and Rocks, Grenoble*, pp 165-179.